

ENERGY AND EXERGY ANALYSIS OF A NOVEL THREE-STAGE HEAT PUMP DRYING SYSTEM

Recep Ekiciler^{1*}

¹ Department of Mechanical Engineering, Faculty of Engineering, Gazi University, 06570, Ankara, Turkey.

Abstract

A three-stage heat pump dryer is analyzed and assessed in terms of energy and exergy performances using different refrigerants such as R134-a, R12, and R22. Many parametric optimization studies are applied for the corresponding system in order to specify the best performing system and environmental parameters. R12 shows the highest energy and exergy efficiencies while requirement of compressor work is low when R12 is used as a refrigerant. The system is not much influenced from the environmental conditions. In addition, the overall system energy and exergy efficiencies are 44.23% and 55.7% for R134-a, respectively.

Keywords: Three-stage heat pump dryer, exergy efficiency, destruction, energy, specific humidity rate.

1. Introduction

The principal purpose of a drying system is to get a dried product of intended quality. Drying is a process in which removal of moisture takes place by energy input. Namely, heat pump drying system is to give the product more heat when compared with environmental conditions. It also energy intensive process. It has a lot of applications such as timber, textile, agriculture, and food. So, there are a lot of studies to improve the efficiency and product quality.

Hodget (1976) firstly investigated heat pump dryer. The efficiency of heat pump dryer was studied. He found that energy consumption is less than comparing the conventional steam heated dryer. In addition, he mentioned the principal of the dehumidifying of heat pump and how its usage could permit improvements in drying efficiency. Cunney & William (1984) studied an engine driven heat pump dryer. They obtained that engine driven heat pump has better performance in term of energy consumption. Meyer & Greyvenstein (1992) performed life cycle cost analysis of a heat pump dryer for drying grain. They argued energy requirement for drying. They also compared different device of energy cost. They conclude that heat pump dryer is more economical than conventional electrical heating device. Söylemez (2006) presented a study about economic analysis of heat pump dryer. He obtained optimum size of components and optimum temperature at optimum minimum life cycle energy cost. Ameen & Bari (2004) investigated whether clothes can be dry or not using waste heat of condenser. They compared that drying rate of the system with trading dryer and drying which occurs at environmental conditions. They found that waste heat of condenser could be utilized for drying. Çolak & Hepbaşlı (2005) investigated the exergy analysis of heat pump drying system. They performed exergy efficiency and exergy destruction for drying of apple. Erbay & İcier (2009) made an optimization to dry olive leaves using heat pump dryer. The purposes of this study are given following order: obtain the effect of some system parameters and optimum working conditions for this system. Gan et al. (2017) investigated an experimental study to understand the effect of temperature and relative humidity on drying of Malaysian bird's nest. They obtained that temperature significantly influences the drying as relative humidity is greater. In addition, energy efficiency of the drying system is high in compared with the other drying system. Erbay & Hepbaşlı (2013) conducted a study about exergy analysis of heat pump dryer. Their purpose is given following: to interpret the exergy performance and to obtain optimum temperature for the system. Furthermore, they determined the exergy destruction rate for each part of the system. Erbay & Hepbaşlı (2014) firstly made an evaluation of exergoeconomic analysis of heat pump drying system. They concluded that heat recovery is one of most effective unit in terms of decreasing total cost of the system. They noticed that when inlet temperature of dryer is decreased, there is an increase cost efficiency of the heat pump dryer. Şevik et al. (2013) investigated to dry mushroom a solar-driven single-stage heat pump drying system. The dryer temperature was changed between 45 °C and 55 °C and air mass flow rate was 310 kg/s. They noticed that coefficient of

***Recep Ekiciler (Corresponding Author):**

Department of Mechanical Engineering, Faculty of Engineering, Gazi University,
06570, Ankara, Turkey. Tel: +90 (312) 582 3430,
E-mail: recepekiciler@gazi.edu.tr

Received : 11.02.2019

Accepted : 24.07.2019

Published : 31.07.2019

performance of the system is ranged 2.1 and 3.1 due to parametric study. Also, they obtained that the product was dried 0.07 g water/g dry product using at least energy. Erbay and Hepbaslı (2017) performed exergoeconomic analysis of ground-source heat pump dryer at different environmental temperatures for the first time. They concluded that condenser is one of most important unit in terms of increasing the total efficiency. Heat exchanger is significantly affected by changing the environmental temperature. Ceylan et al. (2007) conducted an experimental investigation to obtain energy and exergy analysis of timber drying system. They reached that recirculation air ratio depends on the ambient temperature and relative humidity ratio. In addition, they noticed that energy requirement is decreased by decreasing the moisture content in timbers.

There are some modifications on heat pump dryer to enhance the efficiency of heat pump drying system. One of them is two-stage heat pump drying system. It has two different air streams that have different humidity and temperature. This system can ensure multiple purpose like two or more products can be dried (Chua & Chou, 2005). In the literature, there are many studies about two-stage heat pump dryer. Li et al. (2003) performed an experimental study to understand the performance of a system with two evaporators and R-290 as the refrigerant. They found that mass flow rate of R-290 and system's suction pressure increase by the condensing pressure. Brundrett (2013), Rose et al. (1992), Jung and Radermacher (1991), and Simmons et al. (1996) testified the two-stage heat pump dryer superior regarding performance when compared the single-stage heat pump dryer. Namsanguan et al. (2004) experimentally performed two-stage heat pump drying system to decrease the time for drying. The effect of tempering between SSD (superheated steam drying) and HPD (heat pump drying) was investigated. They also compared the steam heated dryer and heat pump dryer. The results showed that SSD/HPD shrimp give lower shrinkage in comparison to the single stage SSD. Zhu et al. (2015) conducted an experimental study to find the effect of the two-stage heat pump drying system. The system was used for drying tobacco. They compared with single-stage and two-stage drying system with respect to drying rate of tobacco. They concluded that two-stage drying system has rate of drying 50% higher than single-stage heat pump drying.

Three-stage heat pump dryer can be used both for drying, heating, and freezing at the same time. However, it is possibly costly to establish it when compared with single or two-stage heat pump dryers. Especially in marine food industry, three-stage heat pump dryer is utilized because of its versatility such as heating, freezing, and drying. Energy and exergy analysis of three-stage heat pump dryer is analyzed for the first time in this study, and the effects of various refrigerants, air humidity and mass flow rate, and ambient conditions on energy and exergy efficiencies are investigated in detail. In addition, exergy efficiencies and exergy destructions are determined for the system components.

2. System Description

A schematic view of the three-stage heat pump dryer is presented in Figure 1. This system has two independent cycles: (1) Air cycle and (2) Refrigerant cycle. Heat pump contains three evaporators, compressors, and expansion valves, a condenser, a sub-cooler, two pressure regulators, two mixers. Three different refrigerants are used for this system such as R134-a, R22, and R12. The refrigerant enters the compressors as saturated vapor and leaves as superheated vapor. The refrigerant entirely condenses at the condenser and entirely evaporates at the evaporators.

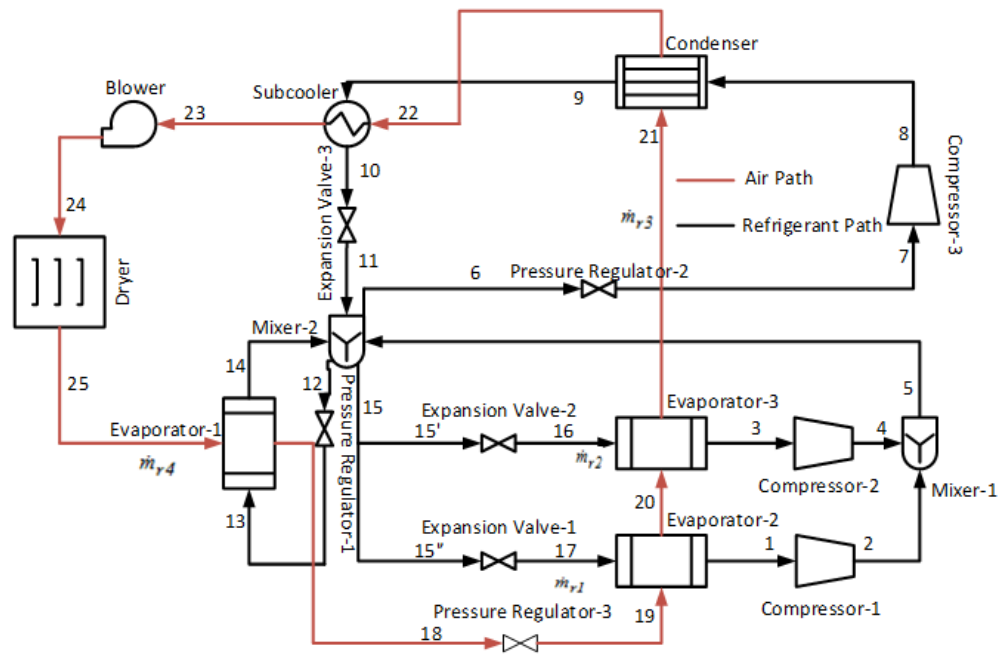


Figure 1. Schematic view of the three-stage heat pump drying system

3. Thermodynamic Analysis

In the system analysis, the effects of the mass flow rate of refrigerant and air, ambient temperature and pressure, compressors pressure ratio, and types of refrigerants on energy and exergy efficiencies are obtained. Also, exergy destruction rate and exergy efficiency is determined for parts of system. For the analysis, the flow is assumed to be steady-state and air is treated as an ideal gas. In addition pressure drops due to frictions and other losses through components and piping are neglected and compressor is taken to be isentropic. Mentioned assumption is made for simplicity of the general assessment of the studied system. Mass, energy, entropy and exergy balances are utilized to determine the energy and exergy efficiencies. The balance equations are given below:

$$\sum_{in} \dot{m} = \sum_{out} \dot{m} \tag{1}$$

$$\sum_{in} (\dot{m}h + \dot{Q} + \dot{W}) = \sum_{out} (\dot{m}h + \dot{Q} + \dot{W}) \tag{2}$$

$$\sum_{in} \dot{m}s + \dot{S}_{gen} + \frac{\dot{Q}_{in}}{T_b} = \sum_{out} \dot{m}s + \frac{\dot{Q}_{out}}{T_0} \tag{3}$$

$$\sum_{in} \dot{m}ex = \sum_{out} \dot{m}ex + \dot{E}x_d + \dot{E}x^Q \tag{4}$$

where h is enthalpy, \dot{m} is mass flow rate, ex is exergy of flow at its state, $\dot{E}x_d$ is exergy destruction rate, and $\dot{E}x^Q$ is thermal exergy rate. Refrigerant and air exergy are calculated as follows, respectively [Rosen et al. (2008), Gaggioli (1980)]:

$$ex_r = (h - h_0) - T_0(s - s_0) \tag{5}$$

$$ex_a = (C_{p,a} + \omega C_{p,v})T_0 [(T/T_0) - 1 - \ln(T/T_0)] + (1 + 1.6078\omega)R_a T_0 \ln(P/P_0) + R_a T_0 \{(1 + 1.6078\omega) + \ln[(1 + 1.6078\omega_0)/(1 + 1.6078\omega)] + 1.6078\omega \ln(\omega/\omega_0)\} \quad (6)$$

where $C_{p,a}$, $C_{p,v}$, R_a , and ω are specific heat of air, specific heat of water vapor, air gas constant and specific humidity ratio, respectively. Thermal exergy is obtained as follows:

$$\dot{Ex}^Q = \dot{Q} \left(1 - \frac{T_L}{T_H} \right) \quad (7)$$

General COP, energy and exergy efficiencies are obtained respectively, as follows:

$$COP_{HP} = \frac{\dot{Q}_{evap}}{\dot{W}_{compressor}} \quad (8)$$

$$\eta = \frac{\dot{E}_{out}}{\dot{E}_{in}} \quad (9)$$

$$\psi = \frac{\dot{Ex}_{useful}}{\dot{Ex}_{in}} \quad (10)$$

Table 1 shows how to determine the exergy destruction rate and exergy efficiency of components as following:

Table 1. Calculation of exergy efficiency and exergy destruction rate of components

COMPONENT	EXERGY EFFICIENCY	EXERGY DESTRUCTION RATE
Compressor-1	$(\dot{E}x_2 - \dot{E}x_1) / W_{comp1}$	$T_0 \dot{m}_{r1} (s_2 - s_1)$
Compressor-2	$(\dot{E}x_4 - \dot{E}x_3) / W_{comp2}$	$T_0 \dot{m}_{r2} (s_4 - s_3)$
Compressor-3	$(\dot{E}x_8 - \dot{E}x_7) / W_{comp3}$	$T_0 \dot{m}_{r3} (s_8 - s_7)$
Mixer-1	$\dot{E}x_5 / (\dot{E}x_4 + \dot{E}x_2)$	$T_0 [(\dot{m}_{r1} + \dot{m}_{r2})s_5 - \dot{m}_{r2}s_4 - \dot{m}_{r1}s_2]$
Mixer-2	$(\dot{E}x_{12} + \dot{E}x_{15} + \dot{E}x_6) / (\dot{E}x_{14} + \dot{E}x_5 + \dot{E}x_{11})$	$T_0 \left[\begin{array}{l} (\dot{m}_{r1} + \dot{m}_{r2})s_{15} + \dot{m}_{r4}s_{12} + \dot{m}_{r3}s_6 \\ -(\dot{m}_{r1} + \dot{m}_{r2})s_5 - \dot{m}_{r3}s_{11} - \dot{m}_{r4}s_{14} \end{array} \right]$
Pressure Regulator-1	$\dot{E}x_{13} / \dot{E}x_{12}$	$T_0 \dot{m}_{r4} (s_{13} - s_{12})$
Pressure Regulator-2	$\dot{E}x_7 / \dot{E}x_6$	$T_0 \dot{m}_{r3} (s_7 - s_6)$
Pressure Regulator-3	$\dot{E}x_{19} / \dot{E}x_{18}$	$T_0 \dot{m}_a (s_{19} - s_{18})$
Expansion Valve-1	$\dot{E}x_{17} / \dot{E}x_{15''}$	$T_0 \dot{m}_{r1} (s_{17} - s_{15''})$
Expansion Valve-2	$\dot{E}x_{16} / \dot{E}x_{15'}$	$T_0 \dot{m}_{r2} (s_{16} - s_{15'})$
Expansion Valve-3	$\dot{E}x_{11} / \dot{E}x_{10}$	$T_0 \dot{m}_{r3} (s_{11} - s_{10})$
Evaporator-1	$(\dot{E}x_{18} + \dot{E}x_{14}) / (\dot{E}x_{13} + \dot{E}x_{25})$	$T_0 [\dot{m}_{r4} (s_{14} - s_{13}) - \dot{m}_a (s_{18} - s_{25})]$
Evaporator-2	$(\dot{E}x_1 + \dot{E}x_{19}) / (\dot{E}x_{19} + \dot{E}x_{17})$	$T_0 [\dot{m}_{r1} (s_1 - s_{17}) - \dot{m}_a (s_{20} - s_{19})]$
Evaporator-3	$(\dot{E}x_3 + \dot{E}x_{21}) / (\dot{E}x_{20} + \dot{E}x_{16})$	$T_0 [\dot{m}_{r2} (s_3 - s_{16}) - \dot{m}_a (s_{21} - s_{20})]$
Sub-cooler	$(\dot{E}x_{10} + \dot{E}x_{23}) / (\dot{E}x_9 + \dot{E}x_{22})$	$T_0 [\dot{m}_{r3} (s_{10} - s_9) - \dot{m}_a (s_{23} - s_{22})]$
Blower	$\dot{E}x_{24} / \dot{E}x_{23}$	$T_0 \dot{m}_a (s_{24} - s_{23})$
Dryer	$\dot{E}x_{25} / \dot{E}x_{24}$	$T_0 \dot{m}_a (s_{25} - s_{24})$
Condenser	$(\dot{E}x_{22} + \dot{E}x_9) / (\dot{E}x_8 + \dot{E}x_{21})$	$T_0 [\dot{m}_{r3} (s_9 - s_8) - \dot{m}_a (s_{22} - s_{21})]$

4. Results and Discussion

Three-stage heat pump dryer is thermodynamically analyzed by using Engineering Equation Solver (EES) in this parametric study. The effect of air and refrigerant, environment temperature and pressure on efficiencies and power consumption of system compressor are investigated in detail. Exergy efficiencies of the components are given for refrigerant 134-a and air in Figure 2. It is revealed that mixer1 (89.9%) has the highest exergy efficiency while mixer 2 (30.52%) has the lowest one. In addition, the some components' exergy efficiencies are in the following order: Dryer 61%, evaporator-1 69.59%, evaporator-2 77.21%, evaporator-3 80.36%, condenser 61.66%, sub-cooler 60.69%, and blower 73.51%.

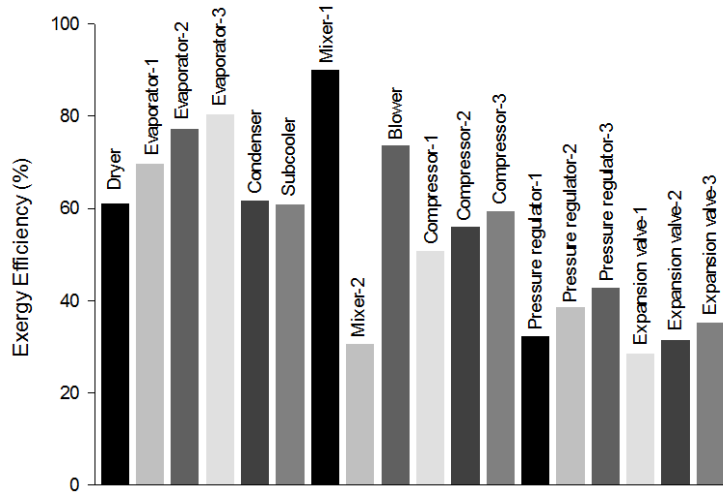


Figure 2. Exergy efficiencies of parts of system for air and R134-a

Exergy destruction rates for system components are illustrated by utilizing R134-a, R12, and R22 in Figure 3(a)-(c). Mass flow rate of air is 0.4 kg/s. According to the system analysis, it is noticed that dryer and blower do not influence from types of refrigerants. Because, air flows in them. In addition, exergy destruction rate for the overall system decreases when R12 is used. R22 has the highest waste of exergy. Exergy destruction rates are obtained in the following ascending order for R134-a: Mixer-1 0.06 kW, condenser 0.1028 kW, blower 0.6107 kW, mixer-2 0.6848 kW, sub-cooler 1.1120 kW, evaporator-2 1.2710 kW, evaporator-3 3.8230 kW, evaporator-1 4.1850 kW, and dryer 6.4110 kW.

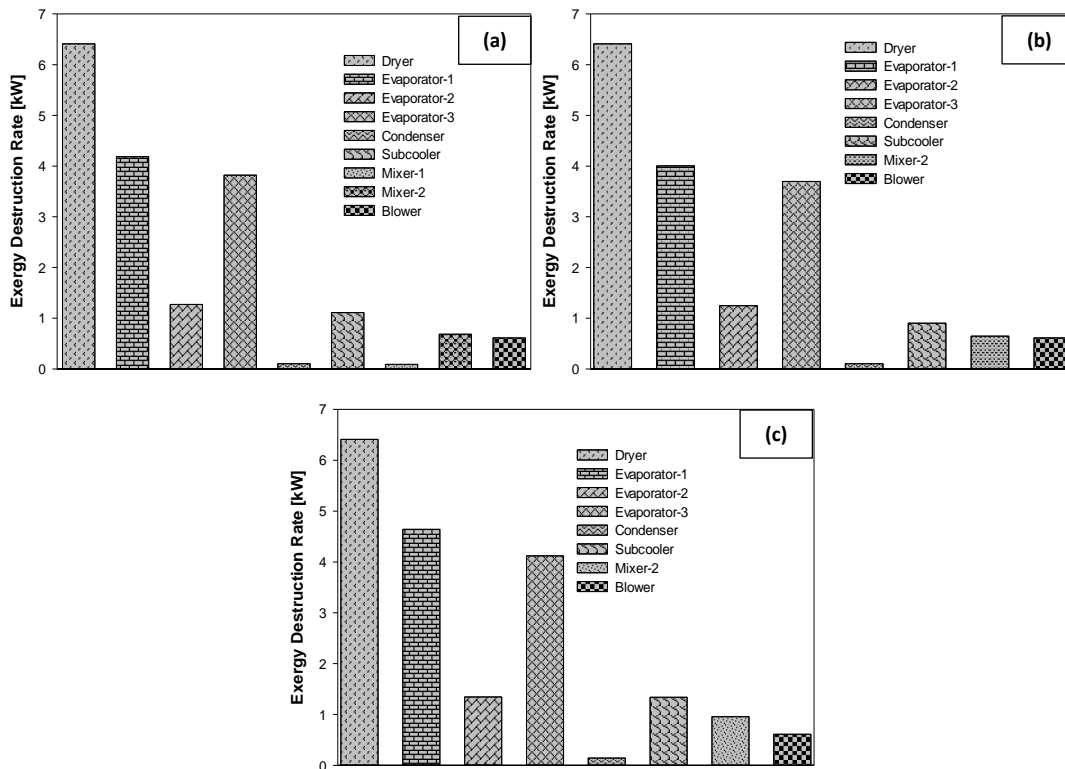


Figure 3. Exergy destruction rates of parts of system using (a) R134-a, (b) R12, (c) R22

Figure 4 represents the effects of the mass flow rate of air on drying unit (dryer, blower, evaporator-1, evaporator-2, evaporator-3, condenser, and sub-cooler) of exergy destruction rate. Mass flow rate of air is chosen such as 0.4 kg/s, 0.6 kg/s, and 0.8 kg/s. It is revealed that exergy destruction rate of all parts of the drying unit increases by increasing mass flow rate of air. When the mass flow rate of air is increased from 0.4 kg/s to 0.6 kg/s, the increment percentage of exergy destruction rate of the dryer, blower, evaporator-1, evaporator-2, evaporator-3, condenser, and sub-cooler are 49%, 50%, 41.6%, 44.8%, 43.5%, 40.17%, and 7.64%, respectively. When the mass flow rate of air is reached 0.8 kg/s, the increment percentage of exergy destruction rate of the drying unit (with the same upper order) are 33.3%, 33.2%, 29.3%, 31%, 30.3%, 28.66%, and 7.1%, respectively. Briefly, it can be concluded that percentage of exergy destruction rate decreases by increasing mass flow rate of air. Furthermore, dryer and blower significantly influence variation of air mass flow rate in comparison to sub-cooler.

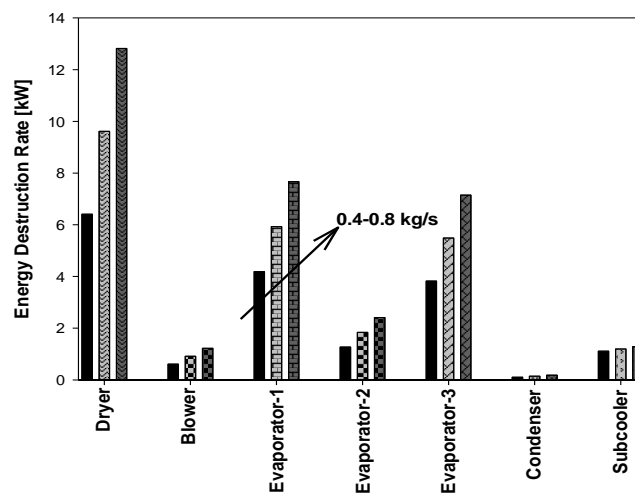


Figure 4. Exergy destruction rates of parts of system using R134-a for different mass flow rate of air

Figure 5 represents the distribution of energy and exergy efficiencies by using R134-a, R12, and R22 for different pressure ratios. It is obtained that energy and exergy efficiencies decrease by increasing pressure ratio for all refrigerants. R12 has the highest efficiencies. The total exergy efficiency increases after pressure ratio of 11 when using R22. The effects of mass flow rate of air on overall energy and exergy efficiencies are exhibited for R134-a, R12, and R22 in Figure 6. Mass flow rate of air is changed between 0.2-0.8 kg/s. The efficiencies show an upward trend for each refrigerant. It is obtained that R12 has the best performance for the three-stage heat pump dryer at the highest mass flow rate of air. Energy efficiency of R134-a and R22 is close each other after mass flow rate of air of 0.5 kg/s.

Energy and exergy efficiencies for various ambient pressure and temperature are almost insignificant. Namely, the heat pump drying system shows similar performance parameters at any season of a year. Figures 7(a)-(c) represent distribution of energy efficiency with various mass flow rate of refrigerants such as R12, R22, and R134-a, respectively. It is noticed that energy efficiency increases with decreasing mass flow rate of R12 and R134-a. Otherwise, energy efficiency increases with increasing mass flow rate of R22. In other words, energy efficiency starts with the value of 41.8% and 39.6% and results with the value of 44.7% and 41.9% for R12 and R134-a, respectively. When the slopes of the Figures 7(a)-(c) is measured, mass flow rate of \dot{m}_{r2} has the lowest effect on energy efficiency for all refrigerants. Variation of mass flow rate of R12, R22, and R134-a effects are investigated on exergy efficiency in Figure 8(a)-(c), respectively. It can be seen from the figures that mass flow rate of refrigerants significantly influences the exergy efficiency. Exergy efficiency increases by decreasing the mass flow rate of refrigerants. Also, \dot{m}_{r2} shows a lower impact when compared to the mass flow rate of \dot{m}_{r1} , \dot{m}_{r3} , and \dot{m}_{r4} on exergy efficiency. Exergy and energy efficiency has the same trend for R12 and R134-a while Exergy and energy efficiency has opposite trend for R22.

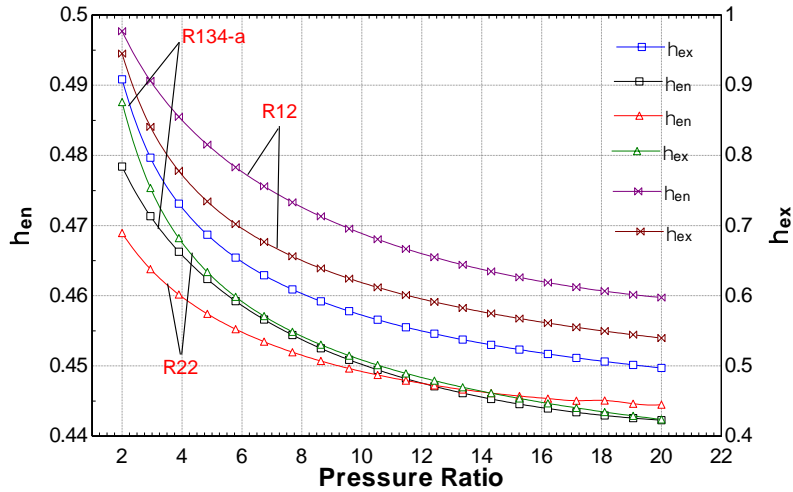


Figure 5. Distribution of overall system energy and exergy efficiencies with pressure ratio for different refrigerants

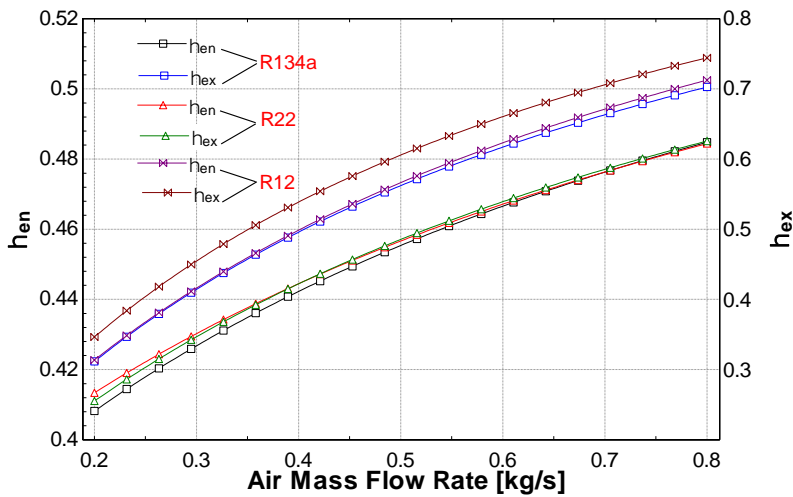
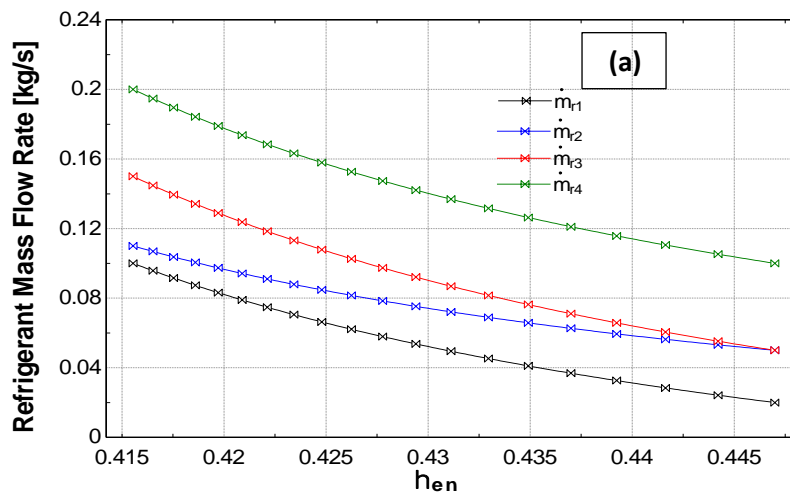


Figure 6. Distribution of overall system energy and exergy efficiencies with mass flow rate of air for different refrigerants



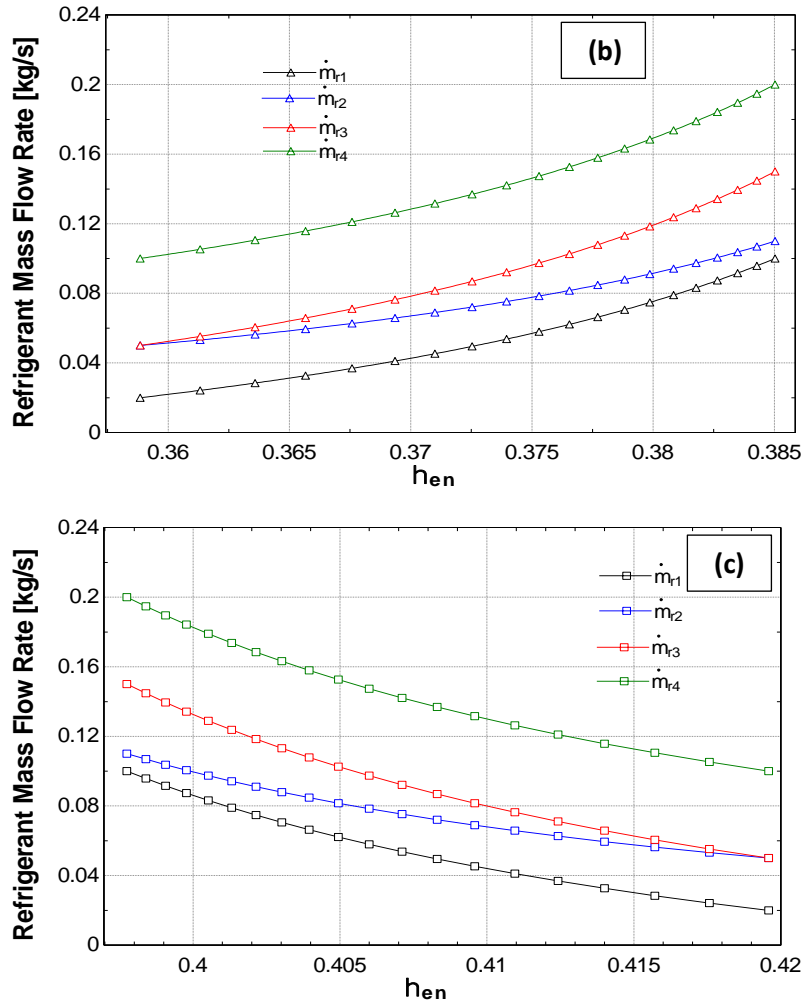
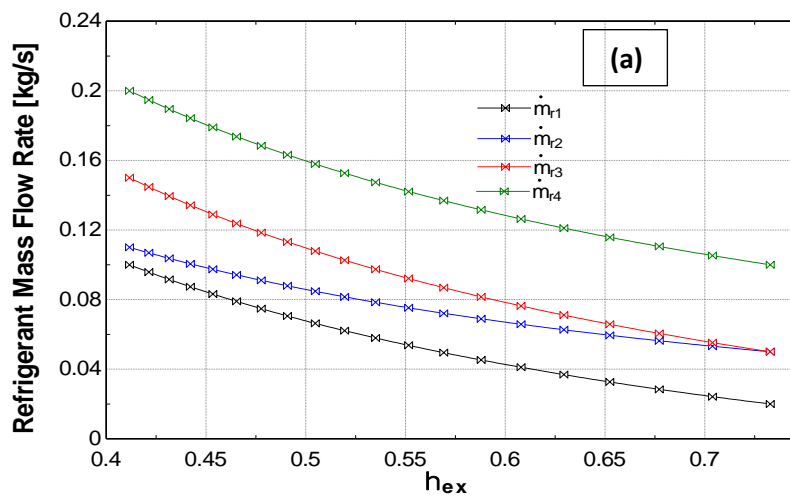


Figure 7. Distribution of overall system energy efficiency with mass flow rate of different refrigerants (a) R12, (b) R22, and (c) R134-a



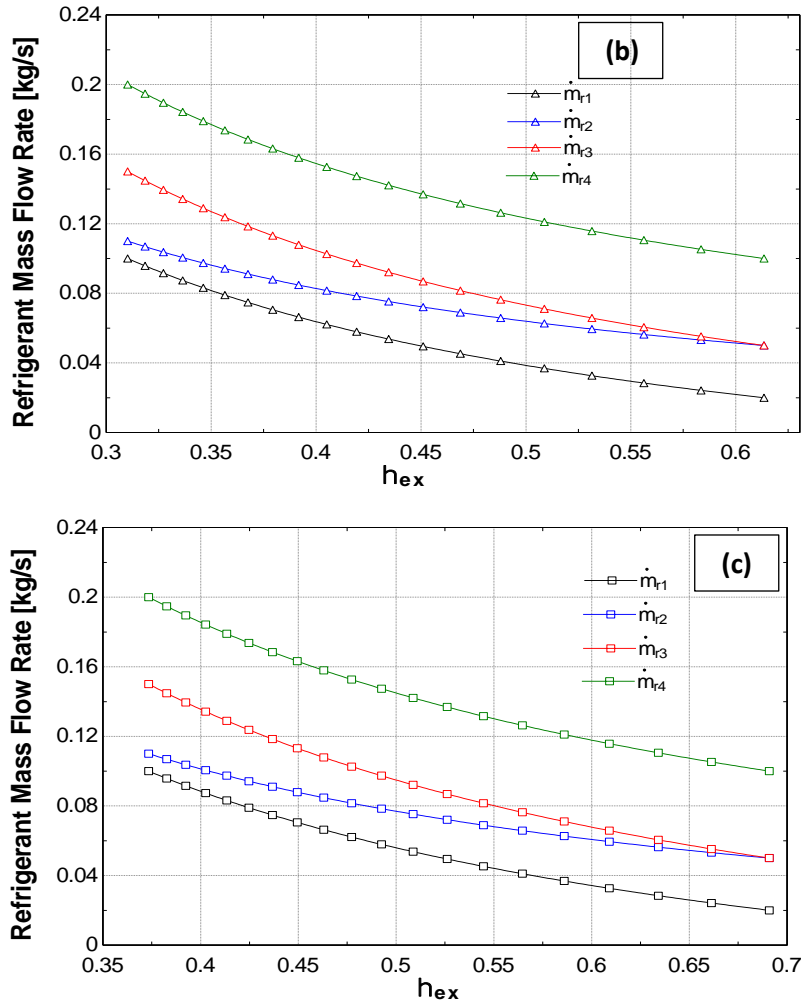


Figure 8. Distribution of overall system exergy efficiency with mass flow rate of different refrigerants (a) R12, (b) R22, and (c) R134-a

Figure 9 represents power consumption of compressor-1, compressor-2, and compressor-3 for R134-a, R12, and R22. It can be concluded that types of refrigerants substantially affect the power consumption of system compressors. It is obtained that power consumptions of compressor-1 are given the following order for R22, R134-a, and R12: 4.024 kW, 3.074 kW, and 2.668 kW. Power consumptions of compressor-2 are determined as 6.437 kW, 4.84 kW, and 4.218 kW for R22, R134-a, and R12. Also, Power consumptions of compressor-3 are calculated as 7.95 kW, 6.297 kW, and 5.407 kW for R22, R134-a, and R12. Power consumption is the lowest value when using R12 for all compressors.

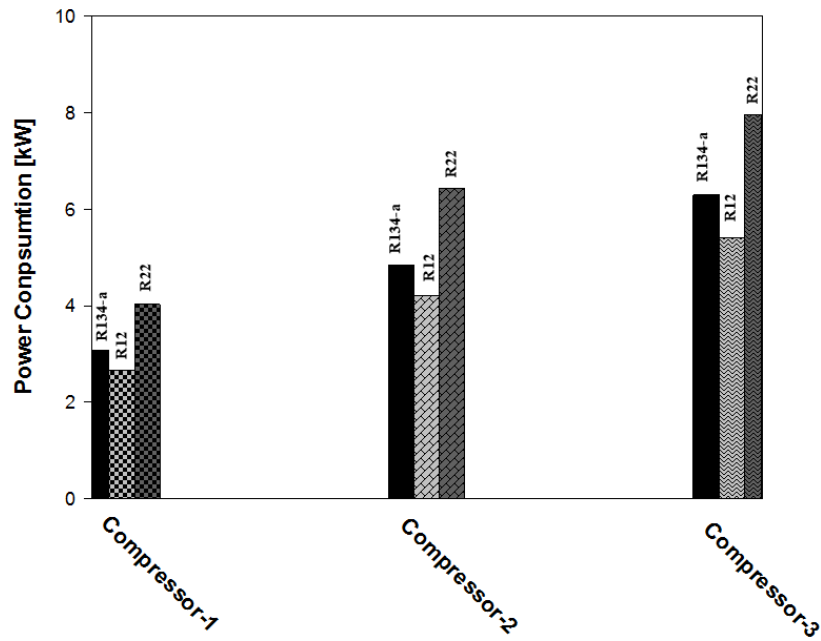


Figure 9. Power consumption distribution of system compressors for different refrigerants

Figure 10, Figure 11, and Figure 12 show power consumption of compressor-1, compressor-2, and compressor-3 with refrigerant mass flow rate for R134-a, R12, and R22. Mass flow rate of refrigerant \dot{m}_{r1} , \dot{m}_{r2} , \dot{m}_{r3} , and \dot{m}_{r4} are changed between 0.02-0.1 kg/s, 0.05-0.11 kg/s, 0.05-0.15 kg/s, and 0.1-0.2 kg/s, respectively. It is observed from the figures that power consumption increases with following order: compressor-1, compressor-2, and compressor-3. Power requirement for compressors linearly increases by increasing mass flow rate of refrigerants. Furthermore, power requirement is significantly influenced by the types of refrigerants. It is revealed that power consumption of compressor is decreased by using R12. R22 has the highest power requirement for triggering the system. On the other hand, R12 has the steepest slope while R22 is exactly the opposite.

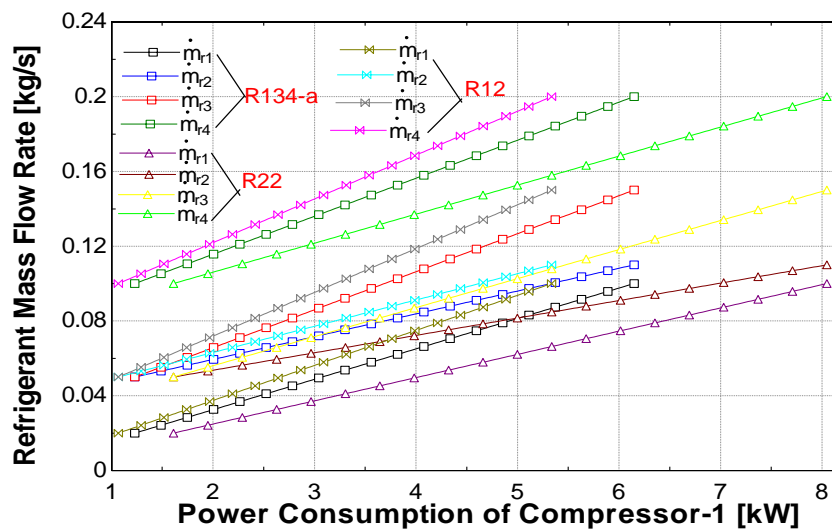


Figure 10. Power consumption distribution of the compressor-1 for different refrigerants

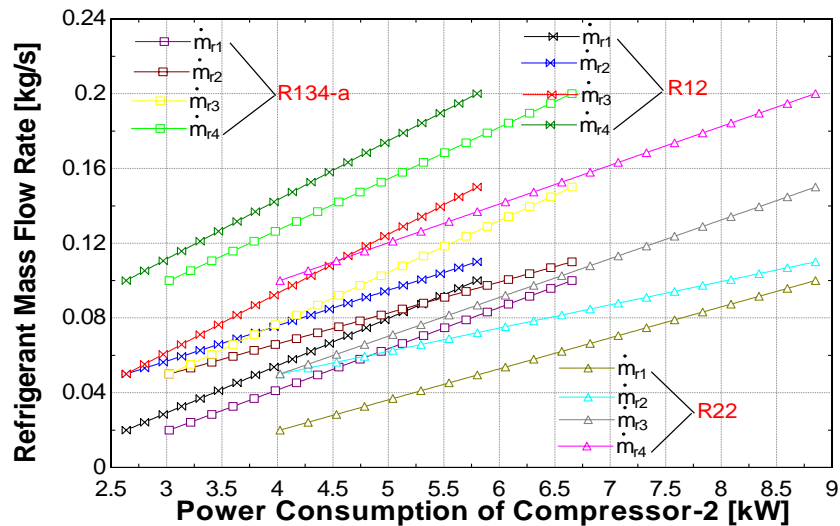


Figure 11. Power consumption distribution of the compressor-2 for different refrigerants

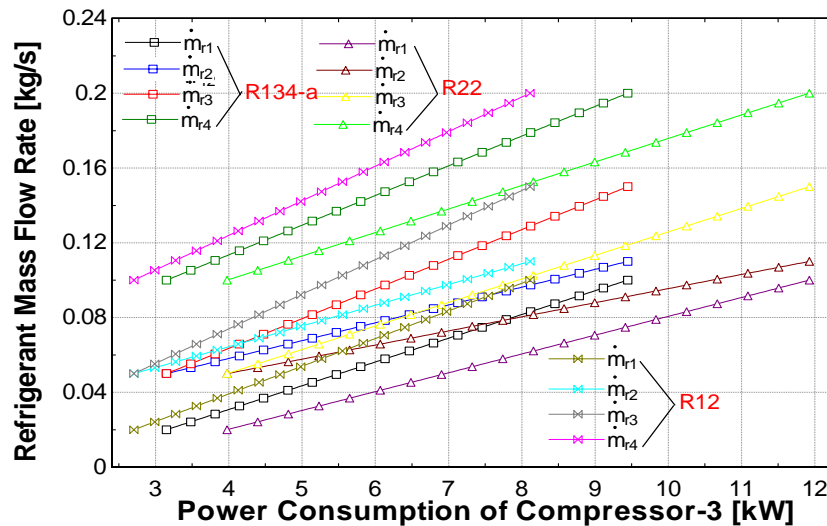


Figure 12. Power consumption distribution of the compressor 3 for different refrigerants

4. Conclusion

A three-stage heat pump drying system is proposed and is investigated in terms of energy and exergy performances. The effects of system are analyzed with respect to ambient temperature and pressure, power consumption of system compressor, and air and refrigerant mass flow rates. Types of refrigerants substantially affect the energy and exergy efficiencies. R12 shows the best performance while R22 represents the lowest performances. The effects of ambient conditions are almost negligible for the studied system. Furthermore, both mass flow rate of air and refrigerants have a key role on energy and exergy efficiencies. In addition, the pressure ratio of compressors is another key factor affecting the efficiency of system. Power requirement of compressors are lowest when using R12 in comparison to R22 and R134-a. The overall system energy and exergy efficiency is 44.23% and 55.7%, respectively. Exergy destruction rate is the highest at dryer.

Nomenclature

C_p : specific heat (kJ/kgK)

COP : coefficient of performance (-)

ex : exergy

$E\dot{x}^Q$: thermal exergy rate (kW)
 $E\dot{x}_d$: exergy destruction rate (kW)
 h : specific enthalpy (kJ/kg)
 \dot{m} : mass flow rate (kg/s)
 P : pressure (kPa)
 R : gas constant (kJ/kgK)
 s : specific entropy (kJ/kgK)
 \dot{S} : entropy (kJ/K)
 T : temperature
 \dot{Q} : thermal energy rate (kW)
 \dot{W} : power (kW)

Greek Symbol

ω : specific humidity rate (kg water/kg air)
 ψ : exergy efficiency (-)
 η : energy efficiency (-)

Subscripts

en : energy
ex : exergy
a : air
r : refrigerant
0 : ambient
b : bulk
gen : generation
in : inlet
out : outlet
L : low
H : high

References

1. **Ameen, A., & Bari, S. (2004)**. Investigation into the effectiveness of heat pump assisted clothes dryer for humid tropics. *Energy Conversion and Management*, 45(9), 1397-1405.
2. **Brundrett, G. W. (2013)**. *Handbook of Dehumidification Technology*. Butterworth-Heinemann.
3. **Ceylan, I., Aktaş, M., & Doğan, H. (2007)**. Energy and exergy analysis of timber dryer assisted heat pump. *Applied Thermal Engineering*, 27(1), 216-222.
4. **Chua, K. J., & Chou, S. K. (2005)**. A modular approach to study the performance of a two-stage heat pump system for drying. *Applied Thermal Engineering*, 25(8), 1363-1379.

5. Colak, N., & Hepbasli, A. (2005). Exergy analysis of drying of apple in a heat pump dryer. In *Second International Conference of the Food Industries and Nutrition Division on Future Trends in Food Science and Nutrition* (pp. 27-29).
6. Cunney, M. B., & Williams, P. (1984). An engine-driven heat pump applied to grain drying and chilling. In G. A. Watts, & J. E. A. Stanbury (Eds.), *Proceedings of the 2nd International Symposium on the Large-Scale Applications of Heat Pumps* (pp. 25-27). Cranfield^ eBedford Bedford: BHRA.
7. Erbay, Z., & Hepbasli, A. (2013). Advanced exergy analysis of a heat pump drying system used in food drying. *Drying Technology*, 31(7), 802-810.
8. Erbay, Z., & Hepbasli, A. (2014). Advanced exergoeconomic evaluation of a heat pump food dryer. *Biosystems Engineering*, 124, 29-39.
9. Erbay, Z., & Hepbasli, A. (2017). Exergoeconomic evaluation of a ground-source heat pump food dryer at varying dead state temperatures. *Journal of Cleaner Production*, 142, 1425-1435.
10. Erbay, Z., & Icier, F. (2009). Optimization of drying of olive leaves in a pilot-scale heat pump dryer. *Drying Technology*, 27(3), 416-427.
11. Gaggioli, R. A. (Ed.). (1980). *Thermodynamics: Second Law Analysis*. American Chemical Society.
12. Gan, S. H., Ong, S. P., Chin, N. L., & Law, C. L. (2017). A comparative quality study and energy saving on intermittent heat pump drying of Malaysian edible bird's nest. *Drying Technology*, 35(1), 4-14.
13. Hodgett, D. L. (1976). Efficient drying using heat pumps. *Chemical Engineer(London)*, (311), 510-12.
14. Jung, D. S., & Radermacher, R. (1991). Performance simulation of a two-evaporator refrigerator— freezer charged with pure and mixed refrigerants. *International Journal of Refrigeration*, 14(5), 254-263.
15. Li, C. J., & Su, C. C. (2003). Experimental study of a series-connected two-evaporator refrigerating system with propane (R-290) as the refrigerant. *Applied Thermal Engineering*, 23(12), 1503-1514.
16. Meyer, J. P., & Greyvenstein, G. P. (1992). The drying of grain with heat pumps in South Africa: A techno-economic analysis. *International Journal of Energy Research*, 16(1), 13-20.
17. Namsanguan, Y., Tia, W., Devahastin, S., & Soponronnarit, S. (2004). Drying kinetics and quality of shrimp undergoing different two-stage drying processes. *Drying Technology*, 22(4), 759-778.
18. Rose, R. J., Jung, D., & Radermacher, R. (1992). Testing of domestic two-evaporator refrigerators with zeotropic refrigerant mixtures. In *ASHRAE Winter Meeting, Anaheim, CA, USA, 01/25-29/92* (pp. 216-225).
19. Rosen, M. A., Dincer, I., & Kanoglu, M. (2008). Role of exergy in increasing efficiency and sustainability and reducing environmental impact. *Energy Policy*, 36(1), 128-137.
20. Simmons, K. E., Haider, I., & Radermacher, R. (1996). Independent compartment temperature control of Lorenz-Meutzner and modified Lorenz-Meutzner cycle refrigerators (No. CONF-960254--). *American Society of Heating, Refrigerating and Air-Conditioning Engineers, Inc.*, Atlanta, GA (United States).
21. Söylemez, M. S. (2006). Optimum heat pump in drying systems with waste heat recovery. *Journal of Food Engineering*, 74(3), 292-298.
22. Şevik, S., Aktaş, M., Doğan, H., & Koçak, S. (2013). Mushroom drying with solar assisted heat pump system. *Energy Conversion and Management*, 72, 171-178.
23. Zhu, W. K., Wang, L., Duan, K., Chen, L. Y., & Li, B. (2015). Experimental and numerical investigation of the heat and mass transfer for cut tobacco during two-stage convective drying. *Drying Technology*, 33(8), 907-914.